Random maps and attractors in random Boolean networks

Björn Samuelsson* and Carl Troein†

Complex Systems Division, Department of Theoretical Physics, Lund University, Sölvegatan 14A, S-223 62 Lund, Sweden
(Received 15 December 2004; revised manuscript received 9 May 2005; published 13 October 2005)

Despite their apparent simplicity, random Boolean networks display a rich variety of dynamical behaviors. Much work has been focused on the properties and abundance of attractors. The topologies of random Boolean networks with one input per node can be seen as graphs of random maps. We introduce an approach to investigating random maps and finding analytical results for attractors in random Boolean networks with the corresponding topology. Approximating some other non-chaotic networks to be of this class, we apply the analytic results to them. For this approximation, we observe a strikingly good agreement on the numbers of attractors of various lengths. We also investigate observables related to the average number of attractors in relation to the typical number of attractors. Here, we find strong differences that highlight the difficulties in making direct comparisons between random Boolean networks and real systems. Furthermore, we demonstrate the power of our approach by deriving some results for random maps. These results include the distribution of the number of components in random maps, along with asymptotic expansions for cumulants up to the fourth order.

I. INTRODUCTION

Random Boolean networks have long enjoyed the attention of researchers, both in their own right and as simplistic models, in particular for gene regulatory networks. These networks are comparatively easy to investigate using computers or analytical methods, yet capable of non-trivial dynamics.

A random Boolean network consists of a number of nodes that each holds a Boolean value (TRUE or FALSE). Every node is associated with a rule, i.e., a Boolean function, that depends on the values of some selected input nodes. The state of all nodes in the network thus gives a Boolean output value for each node, and a node's state can be updated to this value. The network state is evolved with time by repeatedly updating the values, in a temporal order determined by a predefined strategy.

The Boolean rules and their inputs are usually selected at random, drawing from simple distributions. There are several strategies for updating the networks, but most commonly all the nodes are updated at the same time. As with any deterministic scheme, the network dynamics is then fully described by the properties of the relatively small state space. Networks of this kind have been investigated extensively, see, e.g., Refs. [1–7]. In these publications, the link between perturbation propagation and attractor structure has received much attention.

If the network is such that small perturbations tend to die out, the dynamics is said to be ordered or subcritical. For a typical network of this kind, there are relatively few attractors, and a typical attractor is a fixed point or a short cycle. If, on the other hand, perturbations tend to increase with time, the network dynamics is said to be supercritical, and it resembles chaos. Although a deterministic discrete system cannot be truly chaotic, the period of a typical attractor grows exponentially with system size, and the attractors are similar to random walks in the state space. Networks at the borderline, where a small perturbation on average maintains its original size, are said to be critical. The dynamics in such networks lies between the two extremes of ordered and chaotic behavior. In many aspects, the critical case is the most interesting one, where non-trivial results tend to emerge, see, e.g., Ref. [2].

The networks we consider are, generally speaking, such where the inputs to each node are chosen randomly with equal probability among all nodes, and where the Boolean rules of the nodes are picked randomly and independently from some distribution. A prime example is Kauffman networks [1], where all nodes have K inputs and rules are generated with a fixed probability p of returning TRUE for each input state.

In our more general case, realizing a network of N nodes still consists of steps that are taken independently for each node, but from arbitrary, predefined distributions of inputs and rules. There are three steps to be performed for each node:

(a) Pick the number of inputs, called in-degree or connectivity and here denoted K_{in}, from the predefined in-degree distribution.

(b) Pick a Boolean function of K_{in} inputs from the predefined distribution of rules, and let this be the rule of the node.

(c) Pick K_{in} nodes that will serve as the inputs to the rule, giving equal probability to all nodes. This step may either be done without replacement, so that a node can only be chosen once, or with replacement, so that a rule can use the same node for two (or more) of its inputs. In either case, the out-degrees of the nodes will be described by a Poisson distribution when N is large. After a network has been realized, all rules and connections are fixed as the network dynamics is investigated.

_____
*Electronic address: bjorn@thep.lu.se
†Electronic address: carl@thep.lu.se

The network dynamics under consideration is given by synchronous updating of the nodes. At any given time step t, each node has a state of TRUE or FALSE. The state of any node at time $t+1$ is that which its Boolean rule produces when applied to the states of the input nodes at time t. Consequently, the entire network state is updated deterministically, and any trajectory in state space will eventually become periodic. Thus, the state space consists of attractor basins and attractors of varying length, and it always has at least one attractor.

In this work we determine analytically the numbers of attractors of different lengths in networks with connectivity (in-degree) one. We compare these results to networks of higher connectivity and find a remarkable degree of agreement, meaning that networks of single-input nodes can be employed to approximate more complicated networks, even for small systems. For large networks, a reasonable level of correspondence is expected. See Ref. [8] on effective connectivity for critical networks, and Ref. [9] on the limiting numbers of cycles in subcritical networks.

The qualitative results of our analytic derivations can largely be extracted from earlier works, but most of the corresponding quantitative results are new. Although the precise expressions may tell much about dynamics in synchronously updated random Boolean networks with in-degree one, we think that our findings are more valuable in other contexts. First, our approach is not limited to the synchronous updating scheme, nor to Boolean systems. Second, the strong similarities between dynamics in networks with in-degree one and in networks with higher in-degree suggest that valuable understanding of complicated networks may be gained from networks with in-degree one. The second point strengthens the first one considerably, because almost any realistic model will have nodes with connectivity larger than one.

Random Boolean networks with connectivity one have been investigated analytically in earlier work [10,11]. In those papers, a graph-theoretic approach was employed. The approach in Ref. [11] starts with a derivation that also is directly applicable to random maps. For a random Boolean network with connectivity one, a random map can be formed from the network topology. Every node has a rule that takes its input from a randomly chosen node. The operation of finding the input node to a given node forms a map from the set of nodes into itself. This map satisfies the properties of a random map.

For highly chaotic networks, with many inputs per node, the state space can be compared to a random map. Networks where every state is randomly mapped to a successor state are investigated in Ref. [12].

In Ref. [11], only attractors with large attractor basins are considered, and the main results are on the distribution of attractor basin sizes. We extend these calculations and are able to also consider attractors with small attractor basins, and include these in the observables we investigate. Reference [10] focuses on proving superpolynomial scaling, with system size, in the average number of attractors, as well as in the average attractor length, for critical networks with in-degree one. Our calculations reveal more details for cycles of specific lengths.

For long cycles, especially in large networks, there are some artifacts that make direct comparisons to real networks difficult. For example, the integer divisibility of the cycle length is important, see, e.g., Refs. [8,9,11,13,14]. Also, the average number of attractors grows superpolynomially with system size in critical networks [10,13], and most of the attractors have tiny attractor basins as compared to the full state space [6,13,15]. In this work such artifacts become particularly apparent, and we think that long cycles are hard to connect to real dynamical systems.

On the other hand, comparisons to real dynamical systems still seem to be relevant with regard to fixed points and some stability properties [9,16]. An interesting way to make more realistic comparisons regarding cycles is to consider those attractors that are stable with respect to repeated infinitesimal changes in the timing of updating events [17].

Our approach provides a convenient starting point for investigations of random maps in general. Random maps have been the subject of extensive studies, see, e.g., Refs. [18–26], and also Ref. [27] for a book that includes this subject. For networks with in-degree one, our approach enables analytical investigations of far more observables than have been analytically accessible with previously presented methods. This could provide a starting point for understanding more complicated networks, and a tool for seeking observables that may reveal interesting properties in comparisons to real systems.

Several results on random maps can be obtained in a straightforward manner from our approach. One key property of a random map is the number of components in the functional graph, i.e., the number of separated islands in the corresponding network. We rederive a relatively simple expression for the distribution of the number of components, along with asymptotic expansions for cumulants up to the fourth order. To a large extent, the asymptotic results are new.

In Sec. III, we show some numerical comparisons between random Boolean networks of multi-input nodes and networks with connectivity one. The results show similarities that are stronger than we had expected. In future research, it is possible that the connection between networks with single- and multi-input nodes could be better understood by combining our approach with results and ideas from Ref. [14]. In Ref. [14], the connected Boolean networks consisting of one two-input node and an arbitrary number of single-input nodes are investigated. Although there are difficulties in comparing attractor properties directly with real dynamical systems, a satisfactory explanation of the similarities between these networks, with single vs multiple inputs per node, may provide keys to the understanding of dynamics in networks in general.

II. THEORY

In a network with only one-input nodes, the network topology can be described as a set of loops with trees of nodes connected to them. To understand the distribution of attractors of different lengths, it is sufficient to consider the loops. All nodes outside the loops will after a short transient time

act as slaves to the nodes in the loops. Also, the nodes in a loop that contains at least one constant rule, will reach a fixed final state after a short time.

All nodes that are relevant to the attractor structure are contained in loops with only non-constant (information-conserving) rules. In other words, all the relevant elements, as described in Ref. [5], are contained in such loops. We let μ denote the number of information-conserving loops and let $\hat{\mu}$ denote the number of nodes in such loops.

We divide the calculations of the wanted observables into two steps. First, we present general considerations for loop-dependent observables. Then, we apply the general results to investigate observables connected to the attractor structure. Before the second step, we derive expressions for the distributions of μ and $\hat{\mu}$, together with asymptotic expansions for corresponding means and variances, to illustrate the meaning and power of the general expressions.

A. Basic network properties

Throughout this paper, N denotes the number of nodes in the network, and L the length of an attractor, be it a cycle ($L > 1$) or a fixed point ($L = 1$). For brevity we use the term L *cycle*, and understand this to mean an attractor such that taking L time steps forward produces the initial state. When L is the smallest positive integer fulfilling this, we speak of a *proper L cycle*. We denote the number of proper L cycles, for a given network realization, by C_L. The arithmetic mean over realizations of networks of a size N is denoted by $\langle C_L \rangle_N$, so the mean number of network states that are part of a proper L cycle is $L\langle C_L \rangle_N$.

Related to C_L is Ω_L, the number of states that reappear after L time steps and hence are part of any L cycle, proper or not. Analogous to $\langle C_L \rangle_N$, we let $\langle \Omega_L \rangle_N$ denote the average of Ω_L for networks with N nodes. If $\langle \Omega_L \rangle_N$ is known for all L, $\langle C_L \rangle_N$ can be calculated from the set theoretic principle of inclusion-exclusion. See *Supporting Text* to Ref. [9].

For large N, the value of $\langle C_L \rangle_N$ is often misleading, in the sense that some rarely occurring networks with extremely many attractors dominate the average. To better understand this phenomenon, we introduce the observables R_N^L and $\langle \Omega_L \rangle_N^G$. R_N^L denotes the probability that $\Omega_L \neq 0$ for a random network of N nodes, and $\langle \Omega_L \rangle_N^G$ is the geometric mean of Ω_L for N-node networks with $\Omega_L \neq 0$.

In the case that every node has one input, the quantities $\langle \Omega_L \rangle_N$, R_N^L, and $\langle \Omega_L \rangle_N^G$ can be calculated analytically for any N. In the one-input case, the large-N limit of $\langle \Omega_L \rangle_N$, $\langle \Omega_L \rangle_\infty$, is identical to the corresponding limit for subcritical networks of multi-input nodes, as derived in Ref. [9]. Furthermore, we discuss to what extent critical networks of multi-input nodes are expected to show similarities to networks of single-input nodes.

For random Boolean networks of one-input nodes, there are only two relevant control parameters in the model description, apart from the system size N. There are four possible Boolean rules with one input. These are the constant rules, TRUE and FALSE, together with the information-conserving rules that either copy or invert the input. The

distribution of TRUE vs FALSE is irrelevant for the attractor structure of the network. Hence, the relevant control parameters are the probabilities of selecting inverters and copy operators when a rule is randomly chosen. We let r^C and r^I denote the selection probabilities associated with copy operators and inverters, respectively.

In networks with one-input nodes, the total probability of selecting an information-conserving rule is $r \equiv r^C + r^I$. In analogy with the definition of r, we also define $\Delta r \equiv r^C - r^I$. In most cases it is more convenient to work with r and Δr than with r^C and r^I. The quantities r and Δr can also be seen as measures of how a network responds to a small perturbation. From this viewpoint, r and Δr are average growth factors for a random perturbation during one time step. For r, the size of the perturbation is measured with the Hamming distance to an unperturbed network. For Δr, the Hamming distance is replaced by the difference in the number of TRUE values at the nodes.

To get suitable perturbation-based definitions of r and Δr, we consider the following procedure: Find the mean field equilibrium fraction of nodes that have the value TRUE. Pick a random state from this equilibrium as an initial configuration. Let the system evolve one time step, with and without first toggling the value of a randomly selected node. The average fraction of nodes that in both cases copy or invert the state of the selected node are r^C and r^I, respectively. Finally, let $r = r^C + r^I$ and $\Delta r = r^C - r^I$.

It is easy to check that the perturbation-based definitions of r and Δr are consistent with the rule selection probabilities for networks of single-input nodes. By using perturbation-based definitions of r and Δr, those quantities are well-defined for networks with multiple inputs per node [9], and this allows for direct comparisons to networks with one-input nodes.

B. Products of loop observables

In all of our analytical derivations for networks of single-input nodes, we have a common starting point: We consider observables, on the network, that can be expressed as a product of observables associated with the loops in the network.

To make a more precise description, we let $\mathcal{N}$ be any network of single-input nodes, and ν be the number of loops in $\mathcal{N}$. The dynamical properties of a loop are determined by its length $\lambda \in \mathbb{Z}_+$, and a property $s \in \{0, +, -\}$ that we refer to as the sign of the loop. For a loop that does not conserve information, i.e., a loop that has at least one constant node, $s = 0$. All other loops have only inverters and copy operators. If the number of inverters is even then $s = +$, and if it is odd $s = -$.

Let g_λ^s denote a quantity that is fully determined by the length λ and the sign s of a loop. We define the product $G(\mathcal{N})$ of the loop observable g_λ^s in $\mathcal{N}$ as

$$G(\mathcal{N}) \equiv \prod_{i=1}^{\nu} g_{\lambda_i}^{s_i}, \tag{1}$$

where $\lambda_1, \ldots, \lambda_\nu$ and $s_1, \ldots, s_\nu$ are the lengths and signs, respectively, of the loops in the network $\mathcal{N}$.

If the network topology is given, but the rules are randomized independently at each node, the average of $G(\mathcal{N})$ can be calculated according to

$$\langle G \rangle_{\vec{\lambda}} = \prod_{i=1}^{\nu} \langle g \rangle_{\lambda_i}, \tag{2}$$

where $\vec{\lambda} \equiv (\lambda_1, \ldots, \lambda_\nu)$, and $\langle g \rangle_\lambda$ is the average of g_λ^s under random choice of rules.

We proceed by also taking the randomization of the network topology into account. Let ν_λ denote the number of loops of lengths $\lambda = 1, 2, \ldots$, and let $\vec{\nu} \equiv (\nu_1, \nu_2, \ldots)$. Then, the average of $\langle G \rangle_{\vec{\lambda}}$ over network topologies, in networks with N nodes, can be written as

$$\langle G \rangle_N = \sum_{\vec{\nu} \in \mathbb{N}^\infty} P_N(\vec{\nu}) \prod_{\lambda=1}^{\infty} (\langle g \rangle_\lambda)^{\nu_\lambda}, \tag{3}$$

where $P_N(\vec{\nu})$ is the probability that the distribution of loop lengths is described by $\vec{\nu}$ in a network with N nodes. We use infinities in the ranges of the sum and the product for formal convenience. Bear in mind that $P_N(\vec{\nu})$ is nonzero only for such distributions of loop lengths as are achievable with N nodes.

From Ref. [11], we know that

$$P_N(\vec{\nu}) = \frac{\hat{\nu}}{N} \frac{N!}{(N-\hat{\nu})! N^{\hat{\nu}}} \prod_{\lambda=1}^{\infty} \frac{1}{\nu_\lambda! \lambda^{\nu_\lambda}}, \tag{4}$$

where

$$\hat{\nu} \equiv \sum_{\lambda=1}^{\infty} \lambda \nu_\lambda. \tag{5}$$

Equation (4) provides a fundamental starting point for all of our derivations. In its raw form, however, Eq. (4) is difficult to work with. In Appendix A we present how to combine Eq. (4) with Eq. (3), to obtain

$$\langle G \rangle_N = \left. \left(1 + \frac{\partial_z}{N} \right)^N \right|_{z=0} \exp \sum_{\lambda=1}^{\infty} \frac{\langle g \rangle_\lambda - 1}{\lambda} z^\lambda. \tag{6}$$

To continue from Eq. (6), we express $\langle g \rangle_\lambda$ in terms of more fundamental quantities. With r^C and r^I as the probabilities that the rule at any given node is a copy operator or an inverter, respectively, the probability p_λ^+ that a loop of length λ has an even number of inverters is given by

$$p_\lambda^+ = \frac{1}{2}[(r^C + r^I)^\lambda + (r^C - r^I)^\lambda]. \tag{7}$$

Similarly, the probability for an odd number of inverters is given by

$$p_\lambda^- = \frac{1}{2}[(r^C + r^I)^\lambda - (r^C - r^I)^\lambda]. \tag{8}$$

With $r \equiv r^C + r^I$ and $\Delta r \equiv r^C - r^I$, we see that

$$p_\lambda^+ = \frac{1}{2}[r^\lambda + (\Delta r)^\lambda], \tag{9}$$

$$p_\lambda^- = \frac{1}{2}[r^\lambda - (\Delta r)^\lambda], \tag{10}$$

and

$$p_\lambda^0 = 1 - r^\lambda. \tag{11}$$

A loop that does not conserve information will always reach a specific state in a limited number of time steps. Such loops are not relevant for the attractor properties we are interested in. Thus, g_λ^0 should not alter the products, and we have $g_\lambda^0 = 1$. This gives us

$$\langle g \rangle_\lambda = p_\lambda^+ g_\lambda^+ + p_\lambda^- g_\lambda^- + p_\lambda^0 g_\lambda^0 \tag{12}$$

$$= \tilde{g}_\lambda + 1 - r^\lambda, \tag{13}$$

where

$$\tilde{g}_\lambda = \frac{1}{2}[r^\lambda + (\Delta r)^\lambda] g_\lambda^+ + \frac{1}{2}[r^\lambda - (\Delta r)^\lambda] g_\lambda^-. \tag{14}$$

Insertion of Eq. (13) into Eq. (6) and the power series expansion of $\ln(1-x)$ yield

$$\langle G \rangle_N = \left. \left(1 + \frac{\partial_z}{N} \right)^N \right|_{z=0} (1 - rz) \exp \sum_{\lambda=1}^{\infty} \frac{\tilde{g}_\lambda}{\lambda} z^\lambda. \tag{15}$$

Equation (15) is the starting point for all network properties we calculate.

C. Network topology

In this section, we investigate the distributions of the number of information-conserving loops μ and the number of nodes in those loops, $\hat{\mu}$. Both μ and $\hat{\mu}$ are independent of whether the information-conserving loops have positive or negative signs. This means that $g_\lambda^+ = g_\lambda^-$ for all $\lambda = 1, 2, \ldots$. Hence, we let $g_\lambda^\pm \equiv g_\lambda^+ = g_\lambda^-$, and get

$$\tilde{g}_\lambda = g_\lambda^\pm r^\lambda, \tag{16}$$

which means that Eq. (15) turns into

$$\langle G \rangle_N = \left. \left(1 + \frac{\partial_z}{N} \right)^N \right|_{z=0} (1 - rz) \exp \sum_{\lambda=1}^{\infty} \frac{g_\lambda^\pm}{\lambda} (rz)^\lambda. \tag{17}$$

To investigate the distributions of μ and $\hat{\mu}$, we will use *generating functions*. A generating function is a function such that a desired quantity can be extracted by calculating the coefficients in a power series expansion.

Let $[w^k]$ denote the operator that extracts the kth coefficient in a power series expansion of a function of w. Then, the probabilities for specific values of μ and $\hat{\mu}$, in N-node networks, are given by

$$P_N(\mu = k) = [w^k] \langle G \rangle_N, \quad \text{if } g_\lambda^\pm \equiv w \tag{18}$$

and

$$P_N(\hat{\mu} = k) = [w^k] \langle G \rangle_N, \quad \text{if } g_\lambda^\pm \equiv w^\lambda. \tag{19}$$

In Eq. (18), every loop is counted as one, in powers of w, whereas in Eq. (19), every node in each loop corresponds to one factor of w.

For probability distributions described by generating functions, there are convenient ways to extract the statistical moments. Let m denote μ or $\hat{\mu}$. Then, $\langle m \rangle$ and $\langle m^2 \rangle$ can be calculated according to

$$\langle m \rangle = \left. \partial_w \right|_{w=1} \sum_{k=0}^{\infty} P_N(m=k) w^k \qquad (20)$$

$$= \left. \partial_w \right|_{w=1} \langle G \rangle_N \qquad (21)$$

and

$$\langle m^2 \rangle = (1 + \partial_w) \left. \partial_w \right|_{w=1} \sum_{k=0}^{\infty} P_N(m=k) w^k \qquad (22)$$

$$= (1 + \partial_w) \left. \partial_w \right|_{w=1} \langle G \rangle_N. \qquad (23)$$

Starting from Eqs. (18)–(23), we derive some results for μ and $\hat{\mu}$. The derivations are presented in Appendix C. For large N, the probability distribution of μ approaches a Poisson distribution with average $\ln[1/(1-r)]$, whereas the limiting distribution of $\hat{\mu}$ decays exponentially as $P(\hat{\mu}=k) \propto r^k$.

In Appendix C, we also calculate asymptotic expansions for the mean values and variances of μ and $\hat{\mu}$, in the case that $r=1$. The technique to derive asymptotic expansions for products of loop observables is presented in Appendix B.

For $r=1$, μ is equivalent to the number of components in a random map. Similarly, $\hat{\mu}$ corresponds to the size of the invariant set in a random map. The invariant set is the set of all elements that can be mapped to themselves if the map is iterated a suitable number of times. Such elements are located on loops in the network graph.

Using the tools in Appendixes B and C, one can equally well derive asymptotic expansions for higher statistical moments as for the mean and variance. In Sec. III, we state the leading orders of the asymptotic expansions for the third and fourth order cumulants to the distribution of the number of components in a random map.

D. On the number of states in attractors

For a given Boolean network with in-degree one, the number of states Ω_L in L cycles can be expressed as a product of loop observables. If Ω_L is calculated separately for every loop in the network, the product of these quantities gives Ω_L for the whole network.

Every loop with an even number of inverters and length λ can have $2^{\gcd(\lambda,L)}$ states that are repeated after L timesteps, where $\gcd(a,b)$ denotes the greatest common divisor of a and b. Hence, such a loop will contribute with the factor $g_\lambda^+ = 2^{\gcd(\lambda,L)}$ to the product. Similarly, for a loop with an odd number of inverters, this factor is $g_\lambda^- = 2^{\gcd(\lambda,L)}$ if $L/\gcd(\lambda,L)$ is even and $g_\lambda^- = 0$ otherwise. The requirement that $L/\gcd(\lambda,L)$ is even comes from the fact that the state of the loop should be inverted an even number of times during L timesteps.

The condition that $L/\gcd(\lambda,L)$ is even can be reformulated in terms of divisibility by powers of 2. Let $\tilde{\lambda}_L$ denote

the the maximal integer power of 2 such that $\tilde{\lambda}_L | L$, where the relation $|$ means that the number on the left hand side is a divisor to the number on the right hand side. Then, we get

$$L/\gcd(\lambda,L)\,\text{odd} \Leftrightarrow \tilde{\lambda}_L | \lambda. \qquad (24)$$

With

$$g_\lambda^+ = 2^{\gcd(\lambda,L)} \qquad (25)$$

and

$$g_\lambda^- = \begin{cases} 2^{\gcd(\lambda,L)}, & \text{if } \tilde{\lambda}_L \nmid \lambda \\ 0, & \text{if } \tilde{\lambda}_L | \lambda. \end{cases} \qquad (26)$$

inserted into Eq. (14), we get

$$\tilde{g}_\lambda = 2^{\gcd(\lambda,L)} \begin{cases} r^\lambda, & \text{if } \tilde{\lambda}_L \nmid \lambda \\ \dfrac{1}{2}[r^\lambda + (\Delta r)^\lambda], & \text{if } \tilde{\lambda}_L | \lambda. \end{cases} \qquad (27)$$

Now, $\langle \Omega_L \rangle_N$ can be calculated from the insertion of Eq. (27) into Eq. (15). The arithmetic mean, $\langle \Omega_L \rangle_N$, is, however, in many cases a bad measure of Ω_L for a typical network. To see this, we investigate the geometric mean of Ω_L.

We let $\langle \Omega_L \rangle_N^{\mathrm{G}}$ be the geometric mean of nonzero Ω_L, and R_N^L be the probability that $\Omega_L \neq 0$, for networks of size N. The probability distribution of $\log_2 \Omega_L$ is generated by a product of loop observables according to

$$P_N(\log_2 \Omega_L = k) = [w^k]\langle G \rangle_N, \qquad (28)$$

with

$$\tilde{g}_\lambda = w^{\gcd(\lambda,L)} \begin{cases} r^\lambda, & \text{if } \tilde{\lambda}_L \nmid \lambda \\ \dfrac{1}{2}[r^\lambda + (\Delta r)^\lambda], & \text{if } \tilde{\lambda}_L | \lambda. \end{cases} \qquad (29)$$

The probability that $\Omega_L = 0$ is not included in Eq. (28) for $k \in \mathbb{N}$. All other possible values of Ω_L are included, and this means that

$$R_N^L = |_{w=1} \langle G \rangle_N. \qquad (30)$$

Furthermore, it is clear that

$$R_N^L \log_2 \langle \Omega_L \rangle_N^{\mathrm{G}} = R_N^L \langle \log_2 \Omega_L \rangle_N \qquad (31)$$

$$= \left. \partial_w \right|_{w=1} \langle G \rangle_N, \qquad (32)$$

where the average of $\log_2 \Omega_L$ is calculated with respect to networks with $\Omega_L \neq 0$.

Insertion of Eq. (29) into Eq. (15) yields

$$\langle G \rangle_N = \left. \left(1 + \frac{\partial_z}{N}\right)^N \right|_{z=0} F_L(w,z), \qquad (33)$$

where

$$F_L(w,z) = (1 - rz)\exp \sum_{\lambda=1}^{\infty} \frac{w^{\gcd(\lambda,L)}}{\lambda} r^\lambda z^\lambda$$

$$\times \exp \sum_{k=1}^{\infty} \frac{w^{\gcd(k\tilde{\lambda}_L,L)}}{2k\tilde{\lambda}_L}[(\Delta r)^{k\tilde{\lambda}_L} - r^{k\tilde{\lambda}_L}]z^{k\tilde{\lambda}_L}, \tag{34}$$

where $\tilde{\lambda}_L$ is the largest integer power of 2 that divides L.

F_L provides a convenient way to describe our results thus far. We have

$$\langle\Omega_L\rangle_N = \left.\left(1 + \frac{\partial_z}{N}\right)^N\right|_{z=0} F_L(2,z), \tag{35}$$

$$R_N^L = \left.\left(1 + \frac{\partial_z}{N}\right)^N\right|_{z=0} F_L(1,z), \tag{36}$$

and

$$\langle\Omega_L\rangle_N^{\mathrm{G}} = \exp\left[\frac{\ln 2}{R_N^L}\left.\left(1 + \frac{\partial_z}{N}\right)^N \partial_w\right|_{\substack{z=0\\w=1}} F_L(w,z)\right]. \tag{37}$$

Note that $L=0$ can be inserted directly into Eq. (34) to investigate the distribution of the total number of states in attractors. This works because zero is divisible by any nonzero number, and hence $\gcd(\lambda,0)=\lambda$ for all $\lambda \in \mathbb{Z}_+$. Insertion of $L=0$ into Eq. (34), together with standard power series expansions, yields

$$F_0(w,z) = \frac{1 - rz}{1 - rwz}. \tag{38}$$

Equation (38) gives $F_0(1,z)=1$, which means that $R_N^0=1$. The result $R_N^0=1$ is easily understood, because every network must have at least one attractor, and thus a nonzero Ω_0.

The limits $\langle\Omega_L\rangle_\infty$, R_∞^L, and $\langle\Omega_L\rangle_\infty^{\mathrm{G}}$ of $\langle\Omega_L\rangle_N$, R_N^L, and $\langle\Omega_L\rangle_N^{\mathrm{G}}$ as $N\to\infty$ are in many cases easy to extract. For power series of z with convergence radii larger than one, we have the operator relation

$$\lim_{N\to\infty}\left.\left(1 + \frac{\partial_z}{N}\right)^N\right|_{z=0} = \bigg|_{z=1}, \tag{39}$$

which means that the limit can be extracted by letting $z=1$ in the given function. In the cases that fulfill the convergence criterion above, we get

$$\langle\Omega_L\rangle_\infty = F_L(2,1), \tag{40}$$

$$R_\infty^L = F_L(1,1), \tag{41}$$

and

$$\langle\Omega_L\rangle_\infty^{\mathrm{G}} = \exp[\ln 2\,\partial_w|_{w=1}\ln F_L(w,1)]. \tag{42}$$

With one exception, all of Eqs. (40)–(42) hold if $r<1$. The exception is that Eq. (44) does not hold if $L=0$ and $r\geq\frac{1}{2}$.

Using the tools in Appendix B, we find that

$$\langle\Omega_0\rangle_N \approx \begin{cases} \dfrac{1-r}{1-2r}, & \text{for } r < \dfrac{1}{2} \\[2mm] \dfrac{1}{2}\sqrt{\dfrac{\pi}{2}N}, & \text{for } r = \dfrac{1}{2} \\[2mm] \sqrt{\dfrac{\pi}{2}N}e^{[\ln 2r-1+1/(2r)]N}, & \text{for } r > \dfrac{1}{2} \end{cases} \tag{43}$$

and

$$\langle\Omega_0\rangle_N^{\mathrm{G}} \approx \begin{cases} 2^{r/(1-r)}, & \text{for } r < 1 \\[2mm] 2^{\sqrt{\pi N/2}}, & \text{for } r = 1, \end{cases} \tag{44}$$

for large N. Note that the the leading term in the asymptote of $\langle\Omega_0\rangle_N$ for $r>\frac{1}{2}$ comes from the pole in $F_0(2,z)$ at $z=1/(2r)$. If $r>\frac{1}{2}$, then $z=1/(2r)$ lies inside the contour $|z-\frac{1}{3}|=\frac{2}{3}$, which is used as integration path in Appendix B. See Appendixes C and D for examples on how to use the technique presented in Appendix B.

Only if $r<\frac{1}{2}$ do $\langle\Omega_0\rangle_N$ and $\langle\Omega_0\rangle_N^{\mathrm{G}}$ have the same qualitative behavior for large N. Otherwise the broad tail in the distribution of $\hat{\mu}$ dominates the value of $\langle\Omega_0\rangle_N$. If $\frac{1}{2}<r<1$, $\langle\Omega_0\rangle_N^{\mathrm{G}}$ approaches a constant, while $\langle\Omega_0\rangle_N$ grows exponentially with N. For the critical case, $r=1$, the qualitative difference lies in the power of N in the exponent.

For $L\neq 0$, the difference between $\langle\Omega_L\rangle_N$ and $\langle\Omega_L\rangle_N^{\mathrm{G}}$ is less pronounced. Both $\langle\Omega_L\rangle_N$ and $\langle\Omega_L\rangle_N^{\mathrm{G}}$ approach constants as $N\to\infty$ if $r<1$, and they both grow like powers of N if $r=1$. It is also worth noting that $R_\infty^L\neq 0$ for $r<1$, whereas $R_\infty^L=0$ if $r=1$ but $\Delta r<1$. In the latter case, R_N^L approaches zero like $N^{-1/(4\tilde{\lambda}_L)}$; see Appendix D. If $r=1$ and $\Delta r=1$, i.e., the network has only copy operators, $R_N^L=1$ for all $N\in\mathbb{Z}_+$.

In Appendix D, we investigate $\langle\Omega_L\rangle_N$ and $\langle\Omega_L\rangle_N^{\mathrm{G}}$, for $L>0$, in detail for the case that $r=1$ and $\Delta r<1$, which corresponds to the most commonly occurring cases of critical networks. For large N, we have the asymptotic relations

$$\langle\Omega_L\rangle_N \propto N^{U_L} \tag{45}$$

for the arithmetic mean of the number of L cycle states, and

$$\langle\Omega_L\rangle_N^{\mathrm{G}} \propto N^{u_L} \tag{46}$$

for the corresponding geometric mean, with the exponents U_L and u_L given by Eqs. (D23) and (D17) in Appendix D. For large L, we have

$$U_L \approx \frac{2^L}{2L}. \tag{47}$$

The other exponent, u_L, which appears in the scaling of the geometric mean, is trickier to estimate. However, we derive an upper bound from $\varphi(\ell)\leq\ell$, where φ is the Euler function, as described in Appendix D. From this inequality, combined with Eqs. (D17) and (D10), we find that

$$u_L < \frac{\ln 2}{2} d(L), \tag{48}$$

where $d(L)$ is the number of divisors to L. To show that u_L is not bounded for arbitrary L, we let $L=2^m$, where $m \in \mathbb{N}$, and find that $h_L = (m+1)/2$ and

$$u_L = \frac{\ln 2}{8}(m+1). \tag{49}$$

Although $\langle \Omega_L \rangle_N$ and $\langle \Omega_L \rangle_N^G$ share the property that the they grow like powers of N, the values of the powers differ strongly in a qualitative sense. Yet neither case has an upper limit to the exponent in the power law. Thus, the observation that the total number of attractors grows superpolynomially with N is true not only for the arithmetic mean, but also for the geometric mean. This is consistent with the derivations in Ref. [10], that show that the typical number of attractors grows faster than polynomially with N.

III. RESULTS

Our most important findings are the expression for the expectation value of products of loop observables on the graph of a random map [Eq. (15)] and the asymptotic expansions (in Appendix B) for such quantities. Using these tools, we derive new results on basic properties of random maps, and on Boolean dynamics on the graph of a random map. In the latter case, we investigate random Boolean networks with in-degree one, and compare those to more complicated random Boolean networks.

A. Random maps

For critical random Boolean networks with in-degree one, all loops conserve information. This is because no constant Boolean rules are allowed in a critical network. For such a network, the number of information-conserving loops, μ, is also the number of components of the network graph. This graph is also the graph of a random map. Thus, μ can be seen as the number of components in a random map. Analogous to the interpretation of μ, the number of nodes in information-conserving loops, $\hat{\mu}$, can be seen as the number of elements in the invariant set of a random map.

We derive the probability distributions of μ and $\hat{\mu}$, in a form that also can be obtained from other approaches [20,21]. For critical networks, we derive asymptotic expansions for the means and variances of μ and $\hat{\mu}$, and find that

$$\langle \mu \rangle = \frac{1}{2}(\ln 2N + \gamma) + \frac{1}{6}\sqrt{2\pi}N^{-1/2} + O(N^{-1}), \tag{50}$$

$$\sigma^2(\mu) = \frac{1}{2}(\ln 2N + \gamma) - \frac{1}{8}\pi^2 + \frac{1}{6}(3 - 2\ln 2)\sqrt{2\pi}N^{-1/2}$$
$$+ O(N^{-1}), \tag{51}$$

$$\langle \hat{\mu} \rangle = \frac{1}{2}\sqrt{2\pi N} - \frac{1}{3} + \frac{1}{24}\sqrt{2\pi}N^{-1/2} + O(N^{-1}), \tag{52}$$

and

$$\sigma^2(\hat{\mu}) = \frac{1}{2}(4 - \pi)N - \frac{1}{6}\sqrt{2\pi N} - \frac{1}{36}(3\pi - 8) + O(N^{-1/2}), \tag{53}$$

where N is the number of nodes in the network, and γ is the Euler-Mascheroni constant. These expansions converge rapidly to corresponding exact values, for increasing N.

The leading terms $\frac{1}{2}(\ln 2N + \gamma)$ of Eqs. (50) and (51) have been derived earlier. See Refs. [18,28,29] on $\langle \mu \rangle$ and Refs. [28,29] on $\sigma^2(\mu)$. The leading term of Eq. (52) is found in Ref. [28]. The other terms in Eqs. (50)–(53) appear to be new. Some additional terms are presented in Eqs. (C23)–(C26).

The technique presented in Appendix B let us also calculate expansions for cumulants of higher orders. The leading orders of the third and fourth cumulants for the distribution of μ give an interesting hint. Let $\langle \mu^3 \rangle_c$ and $\langle \mu^4 \rangle_c$ denote those cumulants, respectively. Then, we get

$$\langle \mu^3 \rangle_c = \langle \mu \rangle + \frac{7}{4}\zeta(3) - \frac{3}{8}\pi^2 + O(N^{1/2}) \tag{54}$$

and

$$\langle \mu^4 \rangle_c = \langle \mu \rangle + \frac{21}{2}\zeta(3) - \frac{7}{8}\pi^2 - \frac{1}{16}\pi^4 + O(N^{1/2}), \tag{55}$$

where $\zeta(s)$ denotes the Riemann zeta function. All cumulants from the first to the fourth order grow like $\frac{1}{2}\ln N$. One could guess that all cumulants have this property. If so, the distribution of μ is very closely related to a Poisson distribution for large N. (Bear in mind that all cumulants for a Poisson distribution are equal to the average for the distribution.)

Furthermore, it seems like the process of calculating higher order cumulants, as well as including more terms in the expansions, can be fully automated. As far as we know, only a very limited number of terms, and only for mean values and variances, have been derived in earlier work.

B. Random Boolean networks

Our main results from the analytical calculations are the expressions that yield the arithmetic mean $\langle \Omega_L \rangle_N$, and the geometric mean $\langle \Omega_L \rangle_N^G$, of the number of states in L cycles. See Eqs. (34)–(37) on expressions for general N, and Eqs. (40)–(49) on expressions valid for the high-N limit. In Appendix E, we present derivations that relate this work to results from Ref. [9]. These derivations yield an expression suitable for calculation of exact values of $\langle \Omega_L \rangle_N$ via a power series expansion of the function $F_L(2, z)$ in Eq. (35).

For the arithmetic means, the number of proper L cycles $\langle C_L \rangle_N$ can be calculated from the number of states $\langle \Omega_\ell \rangle_N$ in all ℓ cycles, provided that $\langle \Omega_\ell \rangle_N$ is known for all ℓ that divide L. This is done via the inclusion-exclusion principle as described in *Supporting Text* to Ref. [9]. For the corresponding geometric means we cannot use a similar technique, because such means do not have the needed additive properties.

Our results on random Boolean networks are divided into two parts. First, we illustrate our quantitative results on net-

works with in-degree one. To a large extent, the qualitative results are expected from earlier publications.

From Ref. [11], we know that in networks with in-degree one, as $N \to \infty$, the typical number of relevant variables approaches a constant for subcritical networks, and scales as $\sqrt{N}$ for critical networks. This indicates that for subcritical networks, the average number of L cycles and the average number of states in attractors are likely to approach constants as $N \to \infty$.

On the other hand, Ref. [6] points out that the probability distributions of the number of cycles in critical networks have very broad tails. Hence, the arithmetic mean can be much larger than the median of the number of cycles, and this may also be the case for subcritical networks. In Ref. [9], it is found that this effect leads to divergence as $N \to \infty$, in the mean number of attractors, for networks with the stability parameter r in the range $r > \frac{1}{2}$. It is also found that the mean number of cycles of any specific length L converges for large N. For critical networks, it is clear that both the typical number and the mean number of attractors grow superpolynomially with N, in networks with in-degree one [14].

Quantitative results that reflect the above properties for networks of finite sizes are, however, for the most part highly non-trivial to obtain from earlier work. We let Figs. 1–4 illustrate our results in this category. Regarding Fig. 3, it is important to note that the geometric mean of the number of states in attractors can be obtained directly from Ref. [11].

In the second part of our results on random Boolean networks, we compare networks with multi-input nodes to networks with single-input nodes. From a system theoretic viewpoint, this part is the most interesting, because a general understanding of the multi-input effects vs single-input effects in dynamical networks would be very valuable. Although this issue have been addressed before, in, e.g., Refs. [8,11], our results are only partly explained. These results are illustrated in Figs. 5–8.

Figure 1 shows the numbers of attractors of various short lengths as a function of system size, plotted for different values of the stability parameter r. We let $\Delta r = 0$, corresponding to equal probabilities of inverters and copy operators in the networks. For critical networks, with $r = 1$, the asymptotic growth of the average number of proper L cycles, $\langle C_L \rangle_N$, is a power law, while $\langle C_L \rangle_N$ approaches a constant for subcritical networks as N goes to infinity.

For networks with $\Delta r \neq 0$, the prevalences of copy operators and inverters are not identical. Cycles of even length are in general more common then cycles of odd length. An overabundance of inverters strengthens this difference, and conversely a lower fraction of inverters makes the difference less pronounced. See Fig. 2, which shows the symmetric case $\Delta r = 0$ and the extreme cases $\Delta r = \pm r$.

The total number of attractors, $\langle C \rangle_N$, and the total number of states in attractors, $\langle \Omega_0 \rangle_N$, can diverge for large N, even though the number of attractors of any fixed length converges. This is true for subcritical networks with $r > \frac{1}{2}$, and is illustrated in Figs. 3 and 4(a). The growth of $\langle \Omega_0 \rangle_N$ is exponential if $r > \frac{1}{2}$. Interestingly, there is no qualitative difference in the growth of $\langle \Omega_0 \rangle_N$ when comparing the critical case of $r = 1$ to the subcritical ones with $1 > r > \frac{1}{2}$.
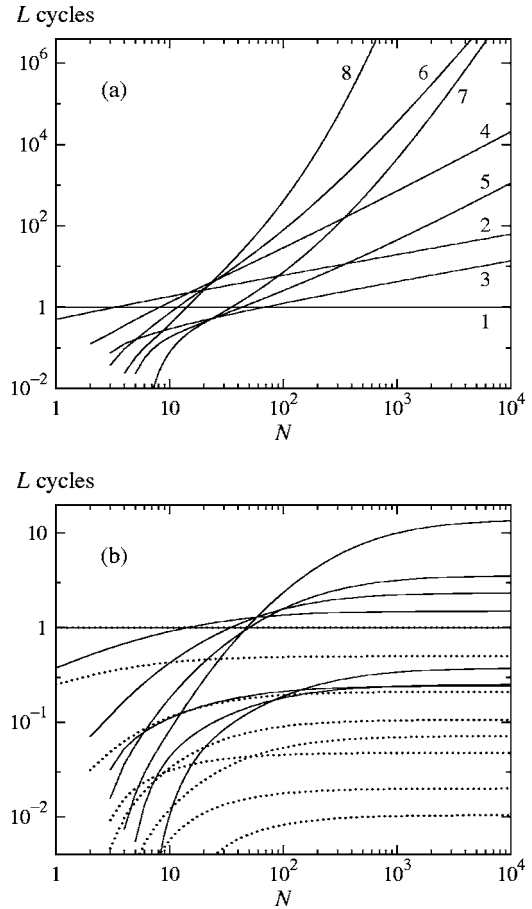

FIG. 1. The average number of proper L cycles as a function of N for different L, for networks with single-input nodes. $r = 1$ in (a), and $r = \frac{3}{4}$ (solid lines), and $r = \frac{1}{2}$ (dotted lines) in (b). In (a), L is indicated in the plot. In (b), L is 3, 5, 7, 1, 2, 4, 6, and 8 for $r = \frac{3}{4}$ and 7, 5, 3, 8, 6, 4, 2, and 1 for $r = \frac{1}{2}$, in that order, from bottom to top along the right boundary of the plot area. In (b), the curves for $L = 3$ and $L = 5$ for $r = \frac{3}{4}$ essentially coincide at the right side of the plot, whereas they split up to the left, with $L = 3$ as the upper curve there.

For $r < \frac{1}{2}$, both $\langle C \rangle_N$ and $\langle \Omega_0 \rangle_N$ converge to constants for large N. In the borderline case $r = \frac{1}{2}$, $\langle \Omega_0 \rangle_N$ diverges like a square root of N, but $\langle C \rangle_N$ seems to approach a constant. See Fig. 4(b).

The number of states in attractors, Ω_0, of a single-input node network is directly related to the total number of nodes, $\hat{\mu}$, that are part of information-conserving loops. Every state of those nodes corresponds to a state in an attractor, and vice versa. Thus, $\Omega_0 = 2^{\hat{\mu}}$, meaning that

$$\langle \Omega_0 \rangle_N = \langle 2^{\hat{\mu}} \rangle \tag{56}$$

and

$$\langle \Omega_0 \rangle_N^G = 2^{\langle \hat{\mu} \rangle}. \tag{57}$$

If $\frac{1}{2} < r \leq 1$, $\ln \langle \Omega_0 \rangle_N$ grows linearly with N. This stands in sharp contrast to $\langle \hat{\mu} \rangle$, which grows like $\sqrt{N}$ for $r = 1$ and approaches a constant for $r < 1$ as $N \to \infty$. Hence, the distri-
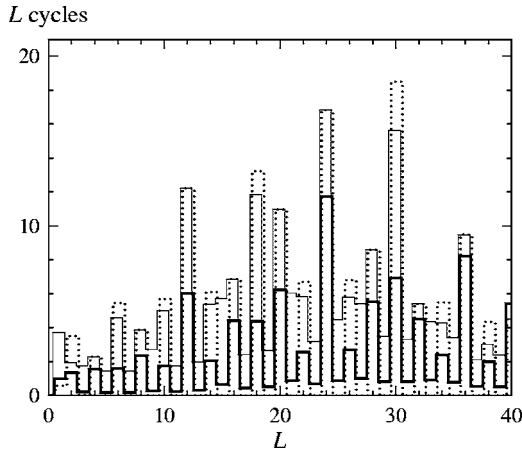
FIG. 2. The average number of proper L cycles for networks (with one-input nodes) with $N=100$ and $r=\frac{3}{4}$, as function of L. $\Delta r=\frac{3}{4}$ (thin solid line), $\Delta r=0$ (thick solid line) and $\Delta r=-\frac{3}{4}$ (dotted line). Note the importance of what numbers divide L.

bution of $\hat{\mu}$ has a broad tail that dominates $\langle \Omega_0 \rangle_N$ if $r > \frac{1}{2}$. This can be understood from the limit distribution of $\hat{\mu}$ for large N. For this distribution, we have $P_\infty(\hat{\mu}=k) \propto r^k$, which means that r must be smaller than $\frac{1}{2}$ for the sum of $2^k P_\infty(\hat{\mu}=k)$ over k to be convergent. Similar, but less dramatic, effects occur when forming averages of Ω_L for $L \neq 0$. The arithmetic mean is in many cases far from the typical value. This is particularly apparent for long cycles in large networks that are critical or close to criticality.

In Ref. [10], it is shown that the typical number of attractors grows superpolynomially with N in critical random Boolean networks with connectivity one. From a different approach, we find the consistent result that $\langle C \rangle_N^G$ grows superpolynomially, where $\langle C \rangle_N^G$ is the geometric mean of the number of attractors. We conclude this from our investigations of the geometric mean of the number of states in L cycles, $\langle \Omega_L \rangle_N^G$. Here, we use the inequality $\langle C \rangle_N^G \geq \langle \Omega_L \rangle_N^G / L$, and the result that there is no upper bound to h_L in the rela-
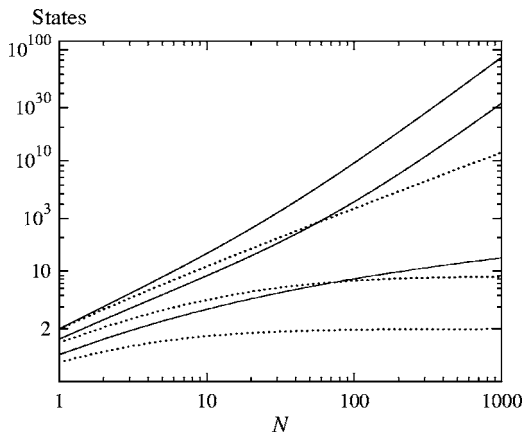

FIG. 3. Arithmetic and geometric means of the number of states, Ω_0, in attractors of networks with one input per node. $\langle \Omega_0 \rangle_N$ (solid lines) and $\langle \Omega_0 \rangle_N^G$ (dotted lines) for $r=\frac{1}{2}$, $r=\frac{3}{4}$ and $r=1$, in that order, from the bottom to the top of the plot. Note that both $\langle \Omega_0 \rangle_N$ and $\langle \Omega_0 \rangle_N^G$ are independent of Δr.
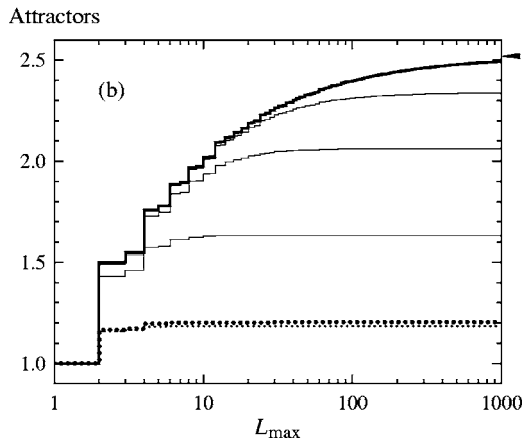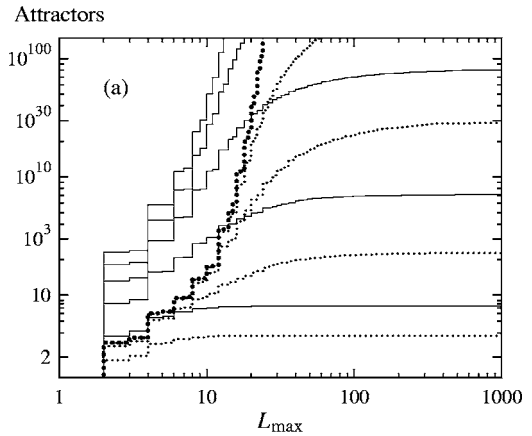

FIG. 4. The arithmetic mean of the number of attractors with lengths $L \leq L_{max}$ in networks with N single-input nodes, for different values of N. In (a) $N=10, 10^2, \ldots, 10^5$ for $r=1$ (thin solid lines) and $N=10, \ldots, 10^4$ for $r=\frac{3}{4}$ (thin dotted lines). In (b) $N=10, 10^2, 10^3$ (thin solid lines) for $r=\frac{1}{2}$ and $N=10$ for $r=\frac{1}{4}$ (thin dotted line). For all cases, $\Delta r=0$. The thick lines in (a) and (b) show the limiting number of attractors when $N \rightarrow \infty$. The arrowhead in (b) marks this limit for $L_{max}=10^7$ for $r=\frac{1}{2}$. The small increase in the number of attractors when L_{max} is changed from 10^3 to 10^7 indicates that $\langle C \rangle_N$ converges when $N \rightarrow \infty$. Note the drastic change in the y-scale between the case $r > \frac{1}{2}$ and $r \leq \frac{1}{2}$.

tion $\langle \Omega_L \rangle_N^G \propto N^{h_L}$, which holds asymptotically for large N [see Eq. (49)].

All the properties above are derived and calculated for networks with one-input nodes, but they seem to a large extent to be valid for networks with multi-input nodes. From Ref. [9], we know that for subcritical networks the limit of $\langle C_L \rangle_N$ as $N \rightarrow \infty$ is only dependent on r and Δr. Hence, we can expect that $\langle C_L \rangle_N$ for a subcritical network with multi-input nodes can be approximated with $\langle C_L \rangle_N'$, calculated for a network with single-input nodes, but with the same r and Δr.

In the networks in Ref. [9] the in-degree of each node is drawn from a power law distribution, and a node cannot have more than one input from any one node. The rules come from a distribution of nested canalizing functions that confer a high degree of stability. For these networks, the single-input approximation fits surprisingly well, as is demonstrated in Fig. 5. Not only are the means of the numbers of attractors
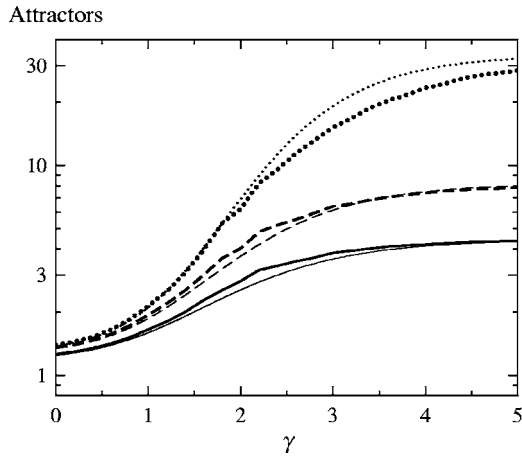
FIG. 5. A comparison between simulations for power law in-degree networks of size $N=20$ (bold lines) and the corresponding networks with single-input nodes (thin lines). The fitted networks have identical values for r, Δr, and N. The solid lines show the number of fixed points, whereas the dashed and dotted lines show the number of two cycles plus fixed points and the total number of attractors, respectively. The probability distribution of in-degrees satisfies $p_K \propto K^{-\gamma}$, where K is the number of inputs. The power law networks use the nested canalyzing rule distribution presented in Ref. [9].

of different types reproduced by this approximation, but the distributions of these numbers are also very similar, as is shown in Fig. 6.

For the critical Kauffman model with in-degree two, we perform an analogous comparison. The number of nodes that are non-constant grows like $N^{2/3}$ for large N [3,13]. Furthermore, the effective connectivity between the non-constant
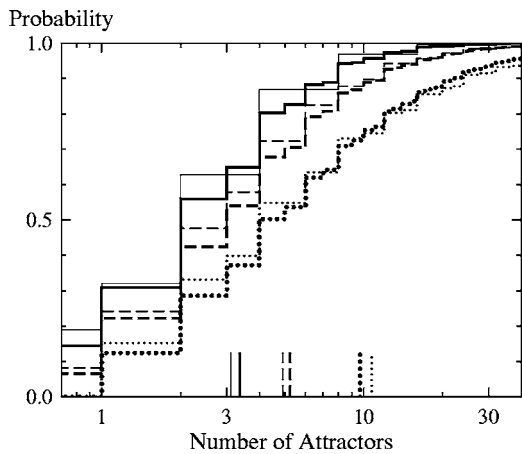

FIG. 6. A cross-section of Fig. 5 at $\gamma=2.5$, with simulation results for the power law in-degree networks (bold lines), and the corresponding single-input networks (thin lines). The distributions of the number of attractors of different types are presented with cumulative probabilities, along with the corresponding means (short vertical lines at the bottom of the plot). The solid lines show the number of fixed points, whereas the dashed and dotted lines show the number of two cycles plus fixed points and the total number of attractors, respectively. Note that the medians are found where the curves for the probability distributions intersect $\frac{1}{2}$ on the y-axis.
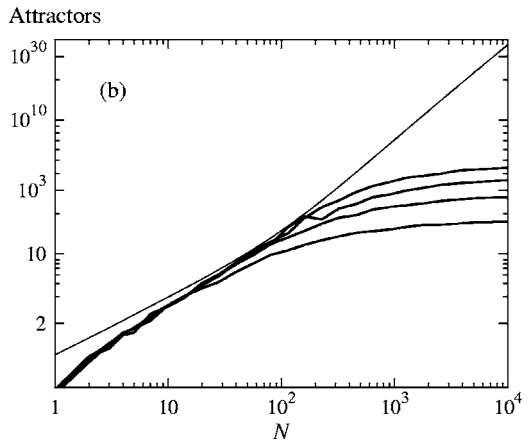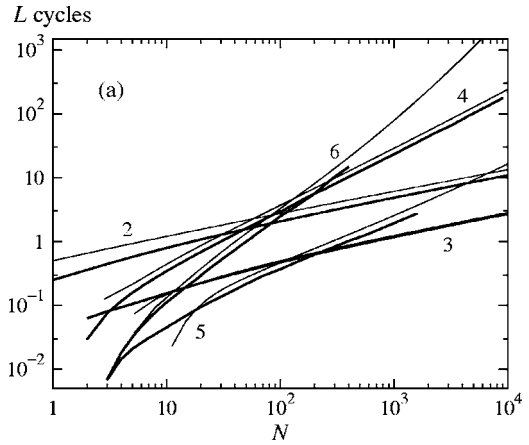

FIG. 7. A comparison between critical $K=2$ Kauffman networks (thick lines) and the corresponding networks of single-input nodes (thin lines). The size of the single-input networks is set to $N' = N^{2/3}$. $r=1$ and $\Delta r=0$, consistent with the Kauffman model. (a) The number of proper L cycles for the L indicated in the plot. For the Kauffman networks, the numbers have been calculated from Monte Carlo summation for those network sizes where could could not be calculated exactly (see Ref. [13]). The number of fixed points is one, independently of N, for both network types. (b) Total number of attractors. This quantity has been calculated analytically for the single-input networks, and estimated by simulations for the Kauffman networks using 10^2, 10^3, 10^4, and 10^5 random starting configurations per network.

nodes approaches one for large N [8]. Hence, one can expect that this type of N-node Kauffman networks can be mimicked by networks with $N' = N^{2/3}$ one-input nodes. For those networks, we choose $r=1$ and $\Delta r=0$, which are the same values as for the Kauffman networks.

For large N, $\langle C_L \rangle_N$ in the Kauffman networks grows like $N^{(H_L-1)/3}$, where H_L is the number of invariant sets of L cycle patterns [13]. For the selected networks with one-input nodes, we have $\langle C_L \rangle'_N \propto N'^{(H_L-1)/2} \propto N^{(H_L-1)/3}$ for large N', see Eq. (D23). This confirms that the choice $N' = N^{2/3}$ is reasonable, but it does not indicate whether the proportionality factor in $N' \propto N^{2/3}$ is anywhere close to one. This factor could also be dependent on L, as can be seen from the calculations in Ref. [13]. However, this initial guess turns out to be surprisingly good, as is shown in Fig. 7(a).
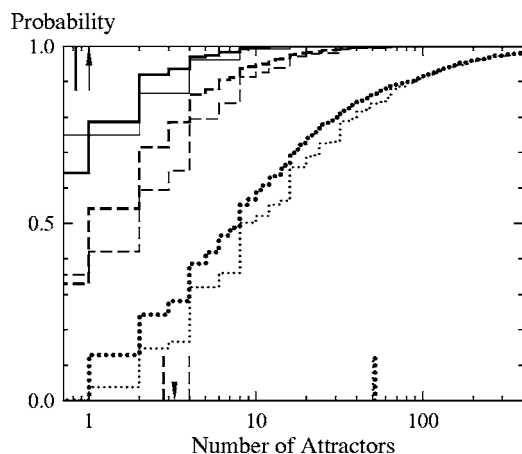
FIG. 8. A cross-section of Fig. 7 at $N=125$, with simulation results for the Kauffman networks (bold lines), and the corresponding single-input networks (thin lines). For the Kauffman networks, we use 10^5 random starting configurations for 1600 network realizations. The corresponding single-input node networks have only $N'=N^{2/3}=25$ nodes, and we perform exhaustive searches through the state space of the relevant nodes in 10^6 such networks. The distributions of the number of attractors of different types are presented with cumulative probabilities, along with the corresponding averages (short vertical lines at the top and bottom of the plot). Corresponding analytical averages, for the Kauffman networks, are marked with arrowheads. The solid lines show the number of fixed points, whereas the dashed and dotted lines show the number of two cycles plus fixed points and the total number of attractors, respectively. Note that the medians are found where the curves for the probability distributions intersect $\frac{1}{2}$ on the y-axis.

From the good agreement for short cycles, one can expect a similar agreement on the mean of the total number of attractors. This is investigated in Fig. 7(b). For networks with up to about 100 nodes, the agreement is good, and the extremely fast growth of $\langle C \rangle'_N$ for larger N is consistent with the slow convergence in the simulations.

As with the power law networks, we also compare the distributions of the numbers of different types of attractors, and find a very strong correspondence. See Fig. 8. Furthermore, we see indications of undersampling, in the estimated numbers of fixed points and two cycles, for the Kauffman networks in Fig. 8, as the means from the simulations are smaller than the corresponding analytical values.

IV. SUMMARY AND DISCUSSION

Using analytical tools, we have investigated random Boolean networks with single-input nodes, along with the corresponding random maps. For random Boolean networks, we extract the exact distributions of the average number of cycles with lengths up to 1000 in networks with up to 10^5 nodes. As has been pointed out in earlier work [6], we see that a small fraction of the networks have many more cycles than a typical network. This property becomes more pronounced as the system size grows, and has drastic effects on the scaling of the average number of states that belong to cycles.

The graph of a random Boolean network of single input nodes can be seen as a graph of a random map. Our analytical approach is not only applicable to Boolean dynamics on such a graph, but also to random maps in general. Using this approach, we rederive some well-known results in a systematic way, and derive some asymptotic expansions with significantly more terms than have been available from earlier publications. In future research, it would be interesting to, e.g., see to what extent the ideas from Ref. [30] and our paper can be combined.

Our results on random Boolean networks highlight some previously observed artifacts. The synchronous updates lead to dynamics that largely is governed by integer divisibility effects. Furthermore, when counting attractors in large networks, most of them are found in highly atypical networks and have attractor basins that are extremely small compared to the full state space. We quantify the role of the atypical networks by comparing arithmetic and geometric means of the number of states in L cycles. From analytical expressions, we find strong qualitative differences between those types of averages.

The dynamics in random Boolean networks with multi-input nodes can to a large extent be understood in terms of the simpler single-input case. In direct comparisons to critical Kauffman networks of in-degree two and to subcritical networks with power law in-degree, the agreement is surprisingly good.

In Ref. [17], a new concept of stability in attractors of Boolean networks is presented. To only consider that type of stable attractors is one way to make more relevant comparisons to real systems. Another way is to focus on fixed points and stability properties as in Refs. [16,9]. Furthermore, the limit of large systems may not always make sense in comparison with real systems. Small Boolean networks may tell more about these than large networks would.

Although there are problems in making direct comparisons between random Boolean networks and real systems, we think that insight into the dynamics of Boolean networks will improve the general understanding of complex systems. For example, can real systems have lots of attractors that are never visited due to small attractor basins, and what implications could such attractors have on the system?

A better understanding of single-input vs multi-input dynamics in Boolean networks could promote a better understanding of similar effects in more complicated dynamical systems. For the random Boolean networks, additional insights are required to properly explain the strong similarities between the single-input and multi-input cases. One interesting issue is to what extent a single-input approximation can be applied to networks with random rules on a fixed network graph.

APPENDIX A: FUNDAMENTAL EXPRESSIONS FOR PRODUCTS OF LOOP OBSERVABLES

Equation (4) inserted into Eq. (3) and a transformation of the summation yield

$$\langle G \rangle_N = \sum_{\vec{\nu} \in \mathbb{N}^\infty} \frac{\hat{\nu}}{N} \frac{N!}{(N-\hat{\nu})! N^{\hat{\nu}}} \prod_{\lambda=1}^\infty \frac{1}{\nu_\lambda!} \left(\frac{\langle g \rangle_\lambda}{\lambda} \right)^{\nu_\lambda} \qquad (A1)$$

$$= \sum_{\nu=1}^\infty \sum_{\vec{\lambda} \in \mathbb{Z}_+^\nu} \frac{\hat{\nu}}{N} \frac{N!}{(N-\hat{\nu})! N^{\hat{\nu}}} \frac{1}{\nu!} \prod_{i=1}^\nu \frac{\langle g \rangle_{\lambda_i}}{\lambda_i}. \qquad (A2)$$

Note that every term in Eq. (A1) is split into $\nu! / \prod_{\lambda=1}^\infty \nu_\lambda!$ equal terms in Eq. (A2).

Define c_N^k according to

$$c_N^k \equiv \frac{N!}{(N-k)! N^k}. \qquad (A3)$$

Then,

$$\langle G \rangle_N = \sum_{\nu=1}^\infty \frac{1}{\nu!} \sum_{\vec{\lambda} \in \mathbb{Z}_+^\nu} (c_N^{\hat{\nu}} - c_N^{\hat{\nu}+1}) \prod_{i=1}^\nu \frac{\langle g \rangle_{\lambda_i}}{\lambda_i}. \qquad (A4)$$

The coefficients c_N^k can be expressed as

$$c_N^k = \left. \left(1 + \frac{\partial_z}{N} \right)^N \right|_{z=0} z^k. \qquad (A5)$$

This relation, together with $\hat{\nu} = \sum_{i=1}^\nu \lambda_i$, inserted into Eq. (A4) gives

$$\langle G \rangle_N = \left. \left(1 + \frac{\partial_z}{N} \right)^N \right|_{z=0} \sum_{\nu=1}^\infty \frac{1}{\nu!} \sum_{\vec{\lambda} \in \mathbb{Z}_+^\nu} (1-z) \prod_{i=1}^\nu \frac{\langle g \rangle_{\lambda_i}}{\lambda_i} z^{\lambda_i}$$

$$= \left. \left(1 + \frac{\partial_z}{N} \right)^N \right|_{z=0} (1-z) \sum_{\nu=1}^\infty \frac{1}{\nu!} \left(\sum_{\lambda=1}^\infty \frac{\langle g \rangle_\lambda}{\lambda} z^\lambda \right)^\nu. \qquad (A6)$$

The outer sum in Eq. (A6) can be modified to start from $\nu = 0$ without altering the value of the expression. This property, together with the power series expansions

$$e^x = \sum_{k=0}^\infty \frac{x^k}{k!} \qquad (A7)$$

and

$$\ln(1-x) = -\sum_{k=1}^\infty \frac{x^k}{k}, \qquad (A8)$$

yields that Eq. (A6) can be rewritten into Eq. (6).

APPENDIX B: ASYMPTOTES FOR PRODUCTS OF LOOP OBSERVABLES

To calculate Eq. (15) for large N, we investigate the operator $(1 + \partial_z / N)^N |_{z=0}$. Let $f(z)$ be a function that is analytic for $z \neq 1$, such that $|z - \frac{1}{3}| \leq \frac{2}{3}$. Furthermore, we assume that $f(z)$ does not have an essential singularity at $z = 1$. Then,

$$\left. \left(1 + \frac{\partial_z}{N} \right)^N \right|_{z=0} f(z) = \left. \frac{\partial_z^N}{N^N} \right|_{z=0} e^{Nz} f(z) \qquad (B1)$$

$$= \frac{N!}{2\pi i} \oint_{C(\epsilon)} dz \frac{e^{Nz}}{z^{N+1}} f(z), \qquad (B2)$$

where ϵ is a small positive number, and $C(\epsilon)$ is the contour of the region where z satisfies $|z - \frac{1}{3}| \leq \frac{2}{3}$ and $|z - 1| \geq \epsilon$.

On the curve $C(\epsilon)$, $|e^{Nz}/z^N|$ is maximal close to $z = 1$, where this expression has a saddle point. Thus, the main contribution to the integral in Eq. (B2), for large N, comes from the vicinity of $z = 1$. Contributions from other parts of $C(\epsilon)$ are suppressed exponentially with N.

To find the asymptotic behavior of Eq. (B2), we perform an expansion of $f(z)$ around $z = 1$ with terms of the form $c[-\ln(1-z)]^m (1-z)^{-a}$, where $a, c \in \mathbb{R}$, and $m \in \mathbb{N}$. Provided that the expansion has a non-zero convergence radius, the asymptote of Eq. (B2) can be determined to any polynomial order of N.

We start at the special case of $f(z) = (1-z)^{-a}$. For non-integral a, $z = 1$ is a branch point of $f(z)$. For such a we let $f(z)$ be real-valued for real $z < 1$ and have a cut line at real $z > 1$. For $N > \max(0, -a)$, we can change the integration path in Eq. (B2). Let $C'(\epsilon)$ follow the line $\text{Re}(z) = 1$ but make a turn about $z = 1$ in the same way as $C(\epsilon)$. Then,

$$\oint_{C(\epsilon)} dz \frac{e^{N(z-1)}}{iz^{N+1}} f(z) = \int_{C'(\epsilon)} dz \frac{e^{N(z-1)}}{iz^{N+1}} f(z). \qquad (B3)$$

From Stirling's formula [31],

$$N! = \frac{n^N}{e^N} \sqrt{2\pi N} \exp\left[\frac{1}{12N} + O(N^{-2}) \right], \qquad (B4)$$

and Eq. (B3), we get

$$\left. \left(1 + \frac{\partial_z}{N} \right)^N \right|_{z=0} f(z) = \sqrt{\frac{N}{2\pi}} \left[1 + \frac{1}{12N} + O(N^{-2}) \right]$$

$$\times \int_{C'(\epsilon)} dz \frac{e^{N(z-1)}}{iz^{N+1}} f(z). \qquad (B5)$$

Around $z = 1$, we have $e^{N(z-1)}/z^N \approx \exp[\frac{1}{2}N(z-1)^2]$. This approximation can be used as a starting point for a suitable expansion. To proceed, we note that we can write

$$\sqrt{\frac{N}{2\pi}} \int_{C'(\epsilon)} \frac{dz}{i} \exp\left[\frac{1}{2} N(z-1)^2 \right] (1-z)^{-a} = Z(a) N^{a/2}, \qquad (B6)$$

where

$$Z(a) \equiv \frac{-i}{\sqrt{2\pi}} \int_{C'(\epsilon)} dz \exp\left[\frac{1}{2}(z-1)^2 \right] (1-z)^{-a}. \qquad (B7)$$

From the fast convergence of $\exp[\frac{1}{2}(z-1)^2]$ along $\text{Re}(z) = 1$ for large $|z|$, it is clear that $a \mapsto Z(a)$ is well defined and continuous for all a.

With $y = 1 - z$, we get

$$\frac{e^{N(z-1)}}{z^{N+1}}(1-z)^{-a} = \exp\{N[-y-\ln(1-y)]\}\frac{y^{-a}}{1-y} \quad \text{(B8)}$$

$$= \exp\left(\frac{1}{2}Ny^2\right)y^{-a}\left[1+y+\frac{1}{3}Ny^3+y^2\right.$$

$$+\frac{7}{12}Ny^4+\frac{1}{18}N^2y^6+y^3+\frac{47}{60}Ny^5$$

$$+\frac{5}{36}N^2y^7+\frac{1}{162}N^3y^9+O(y^4)$$

$$+NO(y^6)+N^2O(y^8)+N^3O(y^{10})$$

$$\left. +\cdots\right]. \quad \text{(B9)}$$

We insert this result into Eq. (B5), and get

$$\left(1+\frac{\partial_z}{N}\right)^N\bigg|_{z=0}(1-z)^{-a} = N^{a/2}\left[\sum_{k=0}^{3}Z_k(a)N^{-k/2}+O(N^{-2})\right], \quad \text{(B10)}$$

where

$$Z_0(a) = Z(a), \quad \text{(B11)}$$

$$Z_1(a) = Z(a-1)+\frac{1}{3}Z(a-3), \quad \text{(B12)}$$

$$Z_2(a) = \frac{1}{12}Z(a)+Z(a-2)+\frac{7}{12}Z(a-4)+\frac{1}{18}Z(a-6), \quad \text{(B13)}$$

and

$$Z_3(a) = \frac{1}{12}Z(a-1)+\frac{37}{36}Z(a-3)+\frac{47}{60}Z(a-5)+\frac{5}{36}Z(a-7)$$

$$+\frac{1}{162}Z(a-9). \quad \text{(B14)}$$

Iterated differentiation of Eq. (B10) with respect to a gives

$$\left(1+\frac{\partial_z}{N}\right)^N\bigg|_{z=0}[-\ln(1-z)]^m(1-z)^{-a}$$

$$= N^{a/2}\left(\frac{1}{2}\ln N+\partial_a\right)^m\left[\sum_{k=0}^{3}Z_k(a)N^{-k/2}+O(N^{-2})\right]. \quad \text{(B15)}$$

It remains for us to calculate $Z(a)$. For $a<1$, Eq. (B7) can be rewritten as

$$Z(a) = \frac{1}{\sqrt{2\pi}}\int_{-\infty}^{\infty}dx\,\exp\left(-\frac{1}{2}x^2\right)(-ix)^{-a}, \quad \text{(B16)}$$

which means that

$$Z(a) = 2^{-a/2}\pi^{-1/2}\cos\left(\frac{1}{2}\pi a\right)\Gamma\left(\frac{1}{2}-\frac{1}{2}a\right) \quad \text{(B17)}$$

for $a<1$. From Eq. (B7) and partial integration, we find that

$$Z(a-2) = (a-1)Z(a), \quad \text{(B18)}$$

which is consistent with Eq. (B17). Hence, Eq. (B17) is valid for all a, provided that the right hand side is replaced with an appropriate limit in case that a is an odd positive integer. The use of the limit is motivated by the continuity of Z.

The recurrence relation in Eq. (B18) is useful for expressing Z_1, Z_2, and Z_3 in more convenient forms. Insertion into Eqs. (B11)–(B14) and factorization of the obtained polynomials gives

$$Z_0(a) = Z(a), \quad \text{(B19)}$$

$$Z_1(a) = \frac{1}{3}(a+1)Z(a-1), \quad \text{(B20)}$$

$$Z_2(a) = \frac{1}{36}a(a+2)(2a-1)Z(a), \quad \text{(B21)}$$

and

$$Z_3(a) = \frac{1}{1620}(a+1)(a+3)(10a^2-15a-1)Z(a-1). \quad \text{(B22)}$$

To express $Z(a)$ in a more convenient form than Eq. (B17), we use the relations

$$\cos x = \prod_{k=0}^{\infty}\left(1-\frac{x^2}{\left(k+\frac{1}{2}\right)^2\pi^2}\right) \quad \text{(B23)}$$

and

$$\Gamma(x) = \frac{e^{\gamma x}}{x}\prod_{k=1}^{\infty}\left(1+\frac{x}{k}\right)e^{x/k}, \quad \text{(B24)}$$

where γ is Euler-Mascheroni constant. See, e.g., Ref. [32] on Eqs. (B23) and (B24). We now get

$$Z(a) = 2^{a/2}e^{a\gamma/2}\prod_{k=0}^{\infty}\left(1+\frac{a}{2k+1}\right)\exp\left(-\frac{a}{2k+1}\right) \quad \text{(B25)}$$

and

$$Z(a) = 2^{a/2}\frac{\Gamma\left(\frac{1}{2}a\right)}{2\Gamma(a)} \quad \text{(B26)}$$

$$= 2^{a/2}\frac{\left(\frac{1}{2}a\right)!}{a!}. \quad \text{(B27)}$$

The first and second order derivatives of $Z(a)$ can be expressed according to

$$Z'(a) = Z(a)\partial_a \ln Z(a) \qquad (B28)$$

and

$$Z''(a) = Z(a)\partial_a^2 \ln Z(a) + Z(a)[\partial_a \ln Z(a)]^2, \qquad (B29)$$

with

$$\partial_a \ln Z(a) = \frac{1}{2}(\ln 2 + \gamma) - \sum_{k=0}^{\infty} \frac{a}{(2k+1)(2k+1+a)} \qquad (B30)$$

and

$$\partial_a^2 \ln Z(a) = -\sum_{k=0}^{\infty} \frac{1}{(2k+1+a)^2}. \qquad (B31)$$

When the values and derivatives of $Z(a)$ are calculated for $a=0$ and $a=1$, one can use the recurrence relation, Eq. (B18), to calculate the corresponding properties for any $a \in \mathbb{Z}$. See, e.g., Ref. [33] on infinite sums that are useful in those derivations.

APPENDIX C: STATISTICS FOR INFORMATION CONSERVING LOOPS

Insertion of Eq. (17) into Eqs. (18) and (19) gives

$$P_N(\mu = k) = [w^k] \left. \left(1 + \frac{\partial_z}{N}\right)^N \right|_{z=0} (1 - rz)^{1-w} \qquad (C1)$$

and

$$P_N(\hat{\mu} = k) = [w^k] \left. \left(1 + \frac{\partial_z}{N}\right)^N \right|_{z=0} \frac{1 - rz}{1 - rwz}. \qquad (C2)$$

An alternative form of the probability generating function in Eq. (C1), for the special case $r=1$, is presented in Ref. [30]. However, this alternative expression is complicated in comparison to Eq. (C1), and it is much easier to extract the probability distribution and corresponding cumulants, along with their asymptotic expansions, from Eq. (C1). In Ref. [30], general considerations for probability generating functions are presented, along with several examples of such functions.

For a power series of z with convergence radius larger than one, we have the operator relation

$$\lim_{N\to\infty} \left.\left(1 + \frac{\partial_z}{N}\right)^N \right|_{z=0} = \Big|_{z=1}, \qquad (C3)$$

which means the limit can be extracted by inserting $z=1$ in the given function. In Eqs. (C1) and (C2), w can be regarded as an arbitrarily small number, which gives arbitrary large convergence radii in the corresponding power expansions in z. Hence, the limiting probabilities for large N are given by

$$P_\infty(\mu = k) = [w^k](1 - r)^{1-w} \qquad (C4)$$

$$= (1 - r)\frac{[-\ln(1 - r)]^k}{k!} \qquad (C5)$$

and

$$P_\infty(\hat{\mu} = k) = [w^k]\frac{1 - r}{1 - rw} \qquad (C6)$$

$$= (1 - r)r^k. \qquad (C7)$$

Both limiting distributions are normalized for $r<1$, but not for $r=1$. This means that the probability distributions remains localized for subcritical networks as N goes to infinity. For critical networks, the probabilities approach zero, which means that the typical values of ν and $\hat{\nu}$ must diverge with N.

Note that Eq. (C5) corresponds to a Poisson distribution with intensity $\ln[1/(1-r)]$, and that the probabilities in Eq. (C7) decay exponentially with rate r. For μ, we get

$$\langle\mu\rangle = \left.\left(1 + \frac{\partial_z}{N}\right)^N \right|_{z=0} [-\ln(1 - rz)] \qquad (C8)$$

$$= \sum_{k=1}^{N} \frac{N!r^k}{k(N-k)!N^k} \qquad (C9)$$

and

$$\langle\mu^2\rangle = \left.\left(1 + \frac{\partial_z}{N}\right)^N \right|_{z=0} \ln(1 - rz)[\ln(1 - rz) - 1] \qquad (C10)$$

$$= \sum_{k=1}^{N} \frac{N!r^k}{k(N-k)!N^k} \left(1 + 2\sum_{j=1}^{k-1} \frac{1}{j}\right). \qquad (C11)$$

If $r=1$, μ can be seen as the number of components in a random map. For random maps, the result in Eq. (C9) is well-known and has been derived in several different ways [18–21]. Alternative derivations of Eq. (C11) are found in Refs. [20,21].

The distribution of μ can be calculated from Eq. (C1). To this end, we consider the series expansion

$$(1 - x)^{-w} = \sum_{n=0}^{\infty} \frac{x^n}{n!} \sum_{k=0}^{n} \begin{bmatrix} n \\ k \end{bmatrix} w^k, \qquad (C12)$$

where $\begin{bmatrix} n \\ k \end{bmatrix}$ are the sign-less Stirling numbers (see, e.g., Ref. [34]). Insertion into Eq. (C1) yields

$$P_N(\mu = k) = \sum_{n=k}^{N} \frac{r^n}{N^n} \binom{N}{n} \left(\begin{bmatrix} n-1 \\ k-1 \end{bmatrix} - \begin{bmatrix} n-1 \\ k \end{bmatrix}\right) \qquad (C13)$$

$$= \sum_{n=k}^{N} \frac{r^n}{N^n} \binom{N}{n} \left(\begin{bmatrix} n \\ k \end{bmatrix} - n\begin{bmatrix} n-1 \\ k \end{bmatrix}\right) \qquad (C14)$$

$$= \sum_{n=k}^{N} \frac{r^n}{N^n} \left(1 - r + \frac{nr}{N}\right) \binom{N}{n} \begin{bmatrix} n \\ k \end{bmatrix}. \qquad (C15)$$

For the number of nodes in information-conserving loops, Eq. (C2) yields

$$P_N(\hat{\mu} = k) = \frac{r^k}{N^k}\left(1 - r + \frac{kr}{N}\right)\binom{N}{k}k!. \tag{C16}$$

For $r=1$, Eq. (C16) is consistent with the corresponding results on the distribution of the number of invariant elements in random maps [19].

Also, Eq. (C16) provides a simpler way to derive Eq. (C15). It is well known that the probability for a random permutation of n to have k cycles is given by

$$\frac{1}{n!}\begin{bmatrix} n \\ k \end{bmatrix}$$

(see, e.g., Ref. [19]). Consider all nodes in information-conserving loops of a Boolean network with in-degree one. We denote the set of such nodes by S. If we randomize the network topology, under the constraint that S is given, the network graph in S will also be the graph of a random permutation of the elements in S. Then, every cycle in this permutation corresponds to an information-conserving loop in the network. In Refs. [21,28], the corresponding observation for random maps was made.

When the network topology is randomized to fit with a given S, only the size $\hat{\mu}$ of S matters. Thus,

$$P_N(\mu = k | \hat{\mu} = n) = \frac{1}{n!}\begin{bmatrix} n \\ k \end{bmatrix}. \tag{C17}$$

Summation over all possible values of $\hat{\mu}$ gives

$$P_N(\mu = k) = \sum_{n=k}^{N} P_N(\mu = k | \hat{\mu} = n) P_N(\hat{\mu} = n), \tag{C18}$$

which together with Eqs. (C16) and (C17) provides a simpler derivation of Eq. (C15). An analogous derivation for random maps is presented in Ref. [21].

For the first and second moments of $\hat{\mu}$, we find that

$$\langle \hat{\mu} \rangle = \left(1 + \frac{\partial_z}{N}\right)^N \bigg|_{z=0} \frac{rz}{1 - rz} \tag{C19}$$

$$= \sum_{k=1}^{N} \frac{N! r^k}{(N-k)! N^k} \tag{C20}$$

and

$$\langle \hat{\mu}^2 \rangle = \left(1 + \frac{\partial_z}{N}\right)^N \bigg|_{z=0} \frac{rz(1 + rz)}{(1 - rz)^2} \tag{C21}$$

$$= \sum_{k=1}^{N} \frac{(2k-1)N! r^k}{(N-k)! N^k}. \tag{C22}$$

To better understand the results on $\langle \mu \rangle$, $\langle \mu^2 \rangle$, $\langle \mu \rangle$, and $\langle \mu^2 \rangle$, we let $r=1$ and calculate their asymptotes for large N. For $r=1$, μ corresponds to the number of components in a random map, while $\hat{\mu}$ corresponds to the number of elements in its invariant set.

From Eq. (B15), we find the large-N asymptotes of $(1+\partial_z/N)^N|_{z=0}$ operating on $-\ln(1-z)$, $[\ln(1-z)]^2$, $(1-z)^{-1}$, and $(1-z)^{-2}$. We also note that $(1+\partial_z/N)^N|_{z=0}1=1$ for all N.

From these asymptotes, combined with Eqs. (C9), (C11), (C20), and (C22) for $r=1$, we get

$$\langle \mu \rangle = \frac{1}{2}(\ln 2N + \gamma) + \frac{1}{6}\sqrt{2\pi}N^{-1/2} - \frac{1}{18}N^{-1}$$

$$- \frac{1}{1080}\sqrt{2\pi}N^{-3/2} + O(N^{-2}), \tag{C23}$$

$$\sigma^2(\mu) = \frac{1}{2}(\ln 2N + \gamma) - \frac{1}{8}\pi^2 + \frac{1}{6}(3 - 2\ln 2)\sqrt{2\pi}N^{-1/2}$$

$$- \frac{1}{18}(\pi - 2)N^{-1} - \frac{1}{3240}(41 - 6\ln 2)\sqrt{2\pi}N^{-3/2}$$

$$+ O(N^{-2}), \tag{C24}$$

$$\langle \hat{\mu} \rangle = \frac{1}{2}\sqrt{2\pi N} - \frac{1}{3} + \frac{1}{24}\sqrt{2\pi}N^{-1/2} - \frac{4}{135}N^{-1} + O(N^{-3/2}), \tag{C25}$$

and

$$\sigma^2(\hat{\mu}) = \frac{1}{2}(4 - \pi)N - \frac{1}{6}\sqrt{2\pi N} - \frac{1}{36}(3\pi - 8) + \frac{17}{1080}\sqrt{2\pi}N^{-1/2}$$

$$+ O(N^{-1}). \tag{C26}$$

Note that the potential term of order $N^{-2}\ln N$ in Eq. (C24) disappears due to cancellation when $\langle \mu \rangle^2$ is subtracted from $\langle \mu^2 \rangle$.

APPENDIX D: ASYMPTOTES RELATED TO BOOLEAN DYNAMICS

We take a closer look at the case that $r=1$ and $\Delta r < 1$. Equation (34) yields

$$F_L(1,z) = \left[\frac{1 - z^{\tilde{\lambda}_L}}{1 - (\Delta rz)^{\tilde{\lambda}_L}}\right]^{1/(2\tilde{\lambda}_L)}. \tag{D1}$$

To the leading order in $1-z$, we get

$$F_L(1,z) = \left[\frac{\tilde{\lambda}_L(1 - z)}{1 - (\Delta rz)^{\tilde{\lambda}_L}}\right]^{1/(2\tilde{\lambda}_L)}[1 + O(1 - z)]. \tag{D2}$$

Insertion into Eqs. (36) and (B10) gives

$$R_N^L = Z\left(\frac{-1}{2\tilde{\lambda}_L}\right)\left[\frac{\tilde{\lambda}_L}{1 - (\Delta r)^{\tilde{\lambda}_L}}\right]^{1/(2\tilde{\lambda}_L)}N^{-1/(4\tilde{\lambda}_L)}[1 + O(N^{-1/2})]. \tag{D3}$$

To find the asymptote of $\langle \Omega_L \rangle_N^G$, we apply Eq. (34) and find that

$$\partial_w|_{w=1}F_L(w,z) = \left(\sum_{\lambda=1}^{\infty} \frac{\gcd(\lambda,L)}{\lambda}z^\lambda - \sum_{k=1}^{\infty} \frac{\gcd(k\tilde{\lambda}_L,L)}{2k\tilde{\lambda}_L} \right.$$

$$\left. \times [1-(\Delta r)^{k\tilde{\lambda}_L}]z^{k\tilde{\lambda}_L} \right) \left[\frac{1-z^{\tilde{\lambda}_L}}{1-(\Delta rz)^{\tilde{\lambda}_L}} \right]^{1/(2\tilde{\lambda}_L)}.$$

$$(D4)$$

Let φ denote the Euler function. The Euler function is defined for $n \in \mathbb{Z}_+$ in such a way that $\varphi(n)$ is the number of values, $k \in \{1,2,\dots,n\}$, that satisfy $\gcd(k,n)=1$. If m divides n, $\varphi(n/m)$ is the number of values, $k \in \{1,2,\dots,n\}$, that satisfy $\gcd(k,n)=m$. From summing over every $m \in \mathbb{N}$ that divides n, we get

$$\sum_{m|n} \varphi(m/n) = n,$$

$$(D5)$$

which means that

$$\sum_{k|n} \varphi(k) = n.$$

$$(D6)$$

From Eq. (D6), we see that

$$\sum_{\lambda=1}^{\infty} \frac{\gcd(\lambda,L)}{\lambda}z^\lambda = -\sum_{\ell|L} \frac{\varphi(\ell)}{\ell} \ln(1-z^\ell).$$

$$(D7)$$

Similarly, we rewrite Eq. (D4) and get

$$\partial_w|_{w=1}F_L(w,z) = \left[\sum_{\ell|L} \frac{\varphi(\ell)}{\ell} \ln \frac{1}{1-z^\ell} \right.$$

$$\left. + \sum_{\ell|L/\tilde{\lambda}_L} \frac{\varphi(\ell)}{2\ell} \ln \frac{1-z^{\ell\tilde{\lambda}_L}}{1-(\Delta rz)^{\ell\tilde{\lambda}_L}} \right]$$

$$\times \left[\frac{1-z^{\tilde{\lambda}_L}}{1-(\Delta rz)^{\tilde{\lambda}_L}} \right]^{1/(2\tilde{\lambda}_L)}.$$

$$(D8)$$

Again, we perform an expansion around $z=1$ and get

$$\partial_w|_{w=1}F_L(w,z) = \left[-\hat{h}_L + \frac{1}{2}(\hat{h}_{L/\tilde{\lambda}_L} + h_{L/\tilde{\lambda}_L} \ln \tilde{\lambda}_L) + s_L \right.$$

$$\left. - \left(h_L - \frac{1}{2}h_{L/\tilde{\lambda}_L} \right) \ln(1-z) \right]$$

$$\times \left[\frac{\tilde{\lambda}_L}{1-(\Delta rz)^{\tilde{\lambda}_L}} \right]^{1/(2\tilde{\lambda}_L)} [1+O(1-z)],$$

$$(D9)$$

where

$$h_L \equiv \sum_{\ell|L} \frac{\varphi(\ell)}{\ell},$$

$$(D10)$$

$$\hat{h}_L \equiv \sum_{\ell|L} \frac{\varphi(\ell)}{\ell} \ln \ell,$$

$$(D11)$$

and

$$s_L \equiv \sum_{\ell|L/\tilde{\lambda}_L} \frac{\varphi(\ell)}{2\ell} \ln \frac{1}{1-(\Delta rz)^{\ell\tilde{\lambda}_L}}.$$

$$(D12)$$

For convenience, we define

$$A_L = -\hat{h}_L + \frac{1}{2}(\hat{h}_{L/\tilde{\lambda}_L} + h_{L/\tilde{\lambda}_L} \ln \tilde{\lambda}_L) + s_L$$

$$(D13)$$

and

$$B_L = h_L - \frac{1}{2}h_{L/\tilde{\lambda}_L}.$$

$$(D14)$$

Insertion of

$$\partial_w|_{w=1}F_L(w,z) = [A_L - B_L \ln(1-z)][1+O(1-z)]$$

$$(D15)$$

into Eq. (37), combined with Eqs. (B15) and (D3), gives

$$\langle \Omega_L \rangle_N^G = \exp \left[(\ln 2) \left(A_L + \frac{1}{2}B_L \ln N + B_L \frac{Z'\left(\frac{-1}{2\tilde{\lambda}_L}\right)}{Z\left(\frac{-1}{2\tilde{\lambda}_L}\right)} \right) \right]$$

$$\times [1+O(N^{-1/2})].$$

$$(D16)$$

This means that $\langle \Omega_L \rangle_N^G$ grows like a power law, N^{u_L}, where the exponent is given by

$$u_L = \frac{\ln 2}{2} \left(h_L - \frac{1}{2}h_{L/\tilde{\lambda}_L} \right).$$

$$(D17)$$

Finally, we derive the asymptote of $\langle \Omega_L \rangle_N$. From Eq. (E4) we get

$$F_L(2,z) = \frac{S_L e^{-\hat{H}_L}}{(1-z)^{H_L-1}}[1+O(1-z)]$$

$$(D18)$$

to the leading order in powers of $1-z$, where

$$H_L \equiv \sum_{\ell|L} J_\ell^+ + \sum_{2\ell|L} J_\ell^-,$$

$$(D19)$$

$$\hat{H}_L \equiv \sum_{\ell|L} J_\ell^+ \ln \ell + \sum_{2\ell|L} J_\ell^- \ln \ell,$$

$$(D20)$$

and

$$S_L \equiv \prod_{\ell|L} \left(\frac{1}{1-(\Delta r)^\ell} \right)^{J_\ell^+} \prod_{2\ell|L} \left(\frac{1}{1+(\Delta r)^\ell} \right)^{J_\ell^-}.$$

$$(D21)$$

The same procedure as for the other asymptotes lets us find the asymptote of Eq. (35). We obtain

$$\langle \Omega_L \rangle_N = S_L e^{-\hat{H}_L} N^{(H_L-1)/2}[1+O(N^{-1})].$$

$$(D22)$$

Hence, $\langle \Omega_L \rangle_N$ grows like a power law, N^{U_L}, where

$$U_L = \frac{H_L - 1}{2}. \tag{D23}$$

Note that H_L is identical to the number of invariant sets of L cycle patterns, as defined in Ref. [13].

APPENDIX E: AN ALTERNATIVE EXPRESSION FOR $F_L(2,z)$

In Ref. [13], we found that

$$\langle \Omega_L \rangle_\infty = (1-r) \prod_{\ell | L} \left(\frac{1}{1-r^\ell} \frac{1}{1-(\Delta r)^\ell} \right)^{J_\ell^+}$$

$$\times \prod_{2\ell | L} \left(\frac{1}{1-r^\ell} \frac{1}{1+(\Delta r)^\ell} \right)^{J_\ell^-}, \tag{E1}$$

where $J_\ell^\pm$ are integers that can be calculated via the inclusion-exclusion principle. J_ℓ^- satisfies the relation

$$2\ell J_\ell^- = \sum_{\mathbf{s} \in \{0,1\}^{\eta_\ell}} (-1)^s 2^{\ell/d_\ell(\mathbf{s})}, \tag{E2}$$

where $s = \sum_{j=1}^{\eta_\ell} s_j$, $d_\ell(\mathbf{s}) = \prod_{j=1}^{\eta_\ell} (d_\ell^j)^{s_j}$, and $d_\ell^1, \ldots, d_\ell^{\eta_\ell}$ are the odd prime divisors to ℓ. Furthermore,

$$J_\ell^+ = J_\ell^- - J_{\ell/2}^-, \tag{E3}$$

where we use the convention that $J_{\ell/2}^- = 0$ for odd ℓ.

From Eq. (E1), we can expect that

$$F_L(2,z) = (1-rz) \prod_{\ell | L} \left(\frac{1}{1-(rz)^\ell} \frac{1}{1-(\Delta rz)^\ell} \right)^{J_\ell^+}$$

$$\times \prod_{2\ell | L} \left(\frac{1}{1-(rz)^\ell} \frac{1}{1+(\Delta rz)^\ell} \right)^{J_\ell^-}. \tag{E4}$$

This is indeed true, and to see that, we rewrite Eq. (E4) via the power series expansion

$$\ln \frac{1}{1-x} = \sum_{k=1}^\infty \frac{1}{k} x^k, \tag{E5}$$

and get

$$F_L(2,z) = (1-rz) \exp \sum_{\ell | L} \sum_{k=1}^\infty \frac{\ell J_\ell^+}{k\ell} [r^{k\ell} + (\Delta r)^{k\ell}] z^{k\ell}$$

$$\times \exp \sum_{2\ell | L} \sum_{k=1}^\infty \frac{\ell J_\ell^-}{k\ell} [r^{k\ell} + (-1)^k (\Delta r)^{k\ell}] z^{k\ell}. \tag{E6}$$

A change of the summation order, with $\lambda = k\ell$, yields

$$F_L(2,z) = (1-rz) \exp \sum_{\lambda=1}^\infty \sum_{\ell | \gcd(\lambda,L)} \frac{\ell J_\ell^+}{\lambda} [r^\lambda + (\Delta r)^\lambda] z^\lambda$$

$$\times \exp \sum_{\lambda=1}^\infty \sum_{\substack{\ell | \gcd(\lambda,L) \\ 2|L/\ell}} \frac{\ell J_\ell^-}{\lambda} [r^\lambda + (-1)^{\lambda/\ell} (\Delta r)^\lambda] z^\lambda. \tag{E7}$$

Equation (E7) is consistent with Eq. (34), provided that

$$\sum_{\ell | \gcd(\lambda,L)} \ell J_\ell^+ + \sum_{\substack{\ell | \gcd(\lambda,L) \\ 2|L/\ell}} \ell J_\ell^- = 2^{\gcd(\lambda,L)} \begin{cases} 1, & \text{if } \widetilde{\lambda}_L \nmid \lambda \\ \frac{1}{2}, & \text{if } \widetilde{\lambda}_L | \lambda, \end{cases} \tag{E8}$$

and

$$\sum_{\ell | \gcd(\lambda,L)} \ell J_\ell^+ + \sum_{\substack{\ell | \gcd(\lambda,L) \\ 2|L/\ell}} (-1)^{\lambda/\ell} \ell J_\ell^- = 2^{\gcd(\lambda,L)} \begin{cases} 0, & \text{if } \widetilde{\lambda}_L \nmid \lambda \\ \frac{1}{2}, & \text{if } \widetilde{\lambda}_L | \lambda. \end{cases} \tag{E9}$$

The sum of Eqs. (E8) and (E9) is given by

$$\sum_{\ell | \gcd(\lambda,L)} 2\ell J_\ell^+ + \sum_{2\ell | \gcd(\lambda,L)} 2\ell J_\ell^- = 2^{\gcd(\lambda,L)}, \tag{E10}$$

which is equivalent to

$$\sum_{\ell | \gcd(\lambda,L)} (2\ell J_\ell^+ + \ell J_{\ell/2}^-) = 2^{\gcd(\lambda,L)} \tag{E11}$$

and

$$\sum_{\ell | \gcd(\lambda,L)} (2\ell J_\ell^- - \ell J_{\ell/2}^-) = 2^{\gcd(\lambda,L)}. \tag{E12}$$

Equation (E12) is true as a consequence of Eq. (E2), and hence Eq. (E10) is true.

The difference between Eqs. (E8) and (E9) is

$$\sum_{\substack{\ell | \gcd(\lambda,L) \\ 2|L/\ell \\ 2|\lambda/\ell}} 2\ell J_\ell^- = 2^{\gcd(\lambda,L)} \begin{cases} 1, & \text{if } \widetilde{\lambda}_L \nmid \lambda \\ 0, & \text{if } \widetilde{\lambda}_L | \lambda \end{cases}. \tag{E13}$$

If $\widetilde{\lambda}_L | \lambda$, the sum in Eq. (E13) is empty and therefore equal to the right hand side. If $\widetilde{\lambda}_L \nmid \lambda$, Eq. (E13) is equivalent to

$$\sum_{\substack{\ell | \gcd(\lambda,L) \\ 2\ell \nmid \gcd(\lambda,L)}} 2\ell J_\ell^- = 2^{\gcd(\lambda,L)}, \tag{E14}$$

consistent with Eq. (E2). Hence, Eq. (E13) holds, and this result concludes the verification of Eqs. (E8) and (E9). Thus, we conclude that Eq. (E4) is correct.

[1] S. A. Kauffman, J. Theor. Biol. **22**, 437 (1969).

[2] M. Aldana-Gonzalez, S. Coppersmith, and L. P. Kadanoff, in *Perspectives and Problems in Nonlinear Science*, edited by E. Kaplan, J. E. Marsden, and K. R. Sreenivasan (Springer, 2003), p. 23.

[3] J. E. S. Socolar and S. A. Kauffman, Phys. Rev. Lett. **90**, 068702 (2003).

[4] B. Derrida and Y. Pomeau, Europhys. Lett. **1**, 45 (1986).

[5] U. Bastolla and G. Parisi, Physica D **115**, 203 (1998).

[6] U. Bastolla and G. Parisi, J. Theor. Biol. **187**, 117 (1997).

[7] H. Flyvbjerg, J. Phys. A **21**, L955 (1988).

[8] U. Bastolla and G. Parisi, Physica D **115**, 219 (1998).

[9] S. Kauffman, C. Peterson, B. Samuelsson, and C. Troein, Proc. Natl. Acad. Sci. U.S.A. **101**, 17102 (2004).

[10] B. Drossel, T. Mihaljev, and F. Greil, Phys. Rev. Lett. **94**, 088701 (2005).

[11] H. Flyvbjerg and H. J. Kjær, J. Phys. A **21**, 1695 (1988).

[12] B. Derrida and H. Flyvbjerg, J. Phys. (Paris) **48**, 971 (1987).

[13] B. Samuelsson and C. Troein, Phys. Rev. Lett. **90**, 098701 (2003).

[14] V. Kaufman and B. Drossel, Eur. Phys. J. B **43**, 115 (2004).

[15] S. Bilke and F. Sjunnesson, Phys. Rev. E **65**, 016129 (2001).

[16] S. Kauffman, C. Peterson, B. Samuelsson, and C. Troein, Proc. Natl. Acad. Sci. U.S.A. **100**, 14796 (2003).

[17] K. Klemm and S. Bornholdt, cond-mat/0411102 (2004).

[18] M. D. Kruskal, Am. Math. Monthly **61**, 392 (1954).

[19] B. Harris, Ann. Math. Stat. **31**, 1045 (1960).

[20] S. M. Ross, J. Appl. Probab. **18**, 309 (1981).

[21] J. Kupka, J. Appl. Probab. **27**, 202 (1990).

[22] L. Katz, Ann. Math. Stat. **26**, 512 (1955).

[23] J. Jaworski, J. Appl. Probab. **21**, 186 (1984).

[24] P. J. Donnelly, W. J. Ewens, and S. Padmadisastra, Adv. Appl. Probab. **23**, 437 (1991).

[25] B. J. English, J. Appl. Probab. **30**, 167 (1993).

[26] J. C. Hansen and J. Jaworski, J. Appl. Probab. **39**, 712 (2002).

[27] B. Bollabás, in *Random Graphs* (Academic Press, London, 1985).

[28] V. E. Stepanov, Theor. Probab. Appl. **14**, 612 (1969).

[29] D. Romero and F. Zertuche, J. Phys. A **36**, 3691 (2003).

[30] H.-K. Hwang, Adv. Appl. Probab. **31**, 448 (1999).

[31] W. Feller, in *An Introduction to Probability Theory and Its Applications*, Vol. 1 (Wiley, New York, 1968).

[32] G. B. Arfken and H. J. Weber, in *Mathematical Methods for Physicists*, 5th ed. (Harcourt/Academic Press, 2001).

[33] I. S. Gradshteyn and I. M. Ryzhik, in *Table of Integrals, Series, and Products* (Academic Press, London, 1965).

[34] C. Berge, in *Principles of Combinatorics* (Academic Press, New York, 1971).